Automotive Experiences
Vol. 5 No. 3 (2022) pp. 477-493
p-ISSN: 2615-6202 e-ISSN: 2615-6636

Review Paper

Mitigation of Porosity and Residual Stress on Car Body Aluminum Alloy Vibration Welding: A Systematic Literature Review

Saifudin[1,2], **Nurul Muhayat**[3], **Eko Surojo**[3], **Yupiter HP Manurung**[4], **Triyono**[3]

[1]Doctoral program in Department of Mechanical Engineering, Universitas Sebelas Maret, 57126, Indonesia
[2]Department of Mechanical Engineering, Universitas Muhammadiyah Magelang, 56172, Indonesia
[3]Department of Mechanical Engineering, Universitas Sebelas Maret, 57126, Indonesia
[4]Faculty of Mechanical Engineering, Universiti Teknologi MARA (UiTM), Shah Alam, Selangor, Malaysia

triyono74@staff.uns.ac.id

https://doi.org/10.31603/ae.7965

Published by Automotive Laboratory of Universitas Muhammadiyah Magelang collaboration with Association of Indonesian Vocational Educators (AIVE)

Article Info
Submitted:
30/09/2022
Revised:
22/11/2022
Accepted:
26/11/2022
Online first:
27/11/2022

Abstract

Fatigue resistance is influenced by porosity and residual stress in welded joints. Fatigue failure in some means of transportation is caused by the inability to withstand the load received from the car body and passengers while operating. This study uses a systematic literature review (SLR) method to identify the effect of vibration welding on porosity and residual stress. Vibration can reduce the empty cavity (porosity) and increase the density of the weld. The ultrasonic vibration spot resistance (UVSR) method with 20 kHz on AA6082 is able to reduce residual stress up to 53% and is effective for homogenization of concentrated residual stress up to 57%.

Keywords: Vibration; Porosity; Residual stress

1. Introduction

In recent decades, aerodynamic design and lightweight vehicle bodies have become the new standard for fuel efficiency purposes [1], [2]. The use of new materials to replace steel such as composite, aluminum or steel/non-steel combinations is the choice of automotive manufacturers to meet new standards [3], [4]. As an alternative vehicle body material, aluminum has many advantages such as; high tensile strength, high corrosion resistance, lightweight, and malleable metal. The specific weight of aluminum is about 2.71 g/cm^3 or about 1/3 of the specific weight of steel, so aluminum is widely used in light vehicles. The lighter the weight of the vehicle, the less energy is needed to move it.

Although aluminum has many advantages as mentioned above, however, aluminum and its alloys have poor weldability. This is due to the properties of aluminum itself such as; a). High thermal conductivity so that it requires a high heat input, b). A large coefficient of expansion so that it is easy for distortion to occur, c). High hydrogen solubility causes porosity. The greater amount of dissolved hydrogen will have an impact on the decrease in ductility properties so that it affects the fracture mode when fatigue failure occurs.

Fatigue is particularly important in welded joints designed for dynamic load structures. Fatigue failure in some means of transportation is caused by the inability to withstand the load received from the car body and passengers while operating. One part with a high risk of fatigue failure is the welded joint between the frame and the car body [5]–[7]. The fatigue resistance will decrease with the formation of porosity in the weld joint [8]. The increasing solubility of hydrogen has a significant role in the weakening of fatigue resistance [9]–[11]. The impact of porosity can cause cracks in the weld, decreased conductivity, and fatigue failure [12], [13]. Fatigue properties are also influenced by residual stresses in welded joints [14], [15]. One way to reduce residual stress is post-weld heat treatment (PWHT) [16]. PWHT is able to increase the fatigue resistance of welded joints [17], [18]. In addition to

PWHT, the vibration stress relieving (VSR) method has been shown to increase the fatigue resistance of welded joints [19], [20]. Although PWHT and VSR are able to reduce residual stresses, the PWHT and VSR methods are less efficient because they require additional work after welding.

The solubility of hydrogen gas occurs in many light alloys which tend to adsorb gas when in a liquid state [21]. The gases that are absorbed by the surface are able to diffuse into the metal on an atomic scale. Hydrogen appears as the only gas that can be dissolved in aluminum and its alloys [22]. The small atomic volume allows hydrogen to diffuse more rapidly into the molten metal than other gases. The solubility of hydrogen is very influential on the mechanical properties of aluminum light alloys, the more the amount of dissolved hydrogen, the mechanical properties of aluminum will decrease [23], [24].

The main problem in welding aluminum alloys is a high susceptibility to the formation of porosity during the solidification process of the weld metal [25], [26]. In welding AA5083 many found problems related to porosity in the weld metal area [27]–[29]. Therefore, the control of the formation of porosity and the effect of the presence of porosity on the weld properties of aluminum and its alloys is a matter of great urgency to be investigated. The problem with dissimilar welding shows that the AA6061 series aluminum alloy has a higher fracture sensitivity than the AA5082 series [30]. The melting point of Magnesium is 651 °C and the boiling point is 1,100 °C, while the melting point of Aluminum Oxide is 2020-2050 °C. Therefore, in the welding process, Mg will evaporate and produce porosity [9]. Aluminum oxide has a much higher melting point than the aluminum base metal which is only around 660 °C. Due to this difference in melting point, during the welding process, the aluminum base metal will melt first while the aluminum oxide layer has not yet melted so the mixing between the aluminum base metal and filler metal is hindered. This can result in incomplete fusion defects in the weld. The aluminum oxide layer is also an insulator that can inhibit the stability of the welding arc flame. In addition, the aluminum oxide that has been contaminated by water vapor (H_2O) will cause a sensation to become Hydrated-oxide alumina (Al_2O_3 H_2O), which is a chemical layer that causes the main cause of porosity.

The next problem is the decrease in the mechanical properties of the HAZ region due to the heat cycle which causes grain coarsening. Dissimilar welding AA5083 and AA6063 are very susceptible 6061 to the formation of porosity that takes place during the solidification process of the weld metal [26].

The porosity of welds on aluminum material occurs as a result of the high solubility of hydrogen gas during welding (solubility of hydrogen) which is quite high [31], [32]. The two main aspects of forming pores are the hydrogen content and the low Mg content [9], [27]. Hydrogen can arise from welding electrodes, workpiece material, environment and air [33], [34]. The solubility of hydrogen gas occurs in many light alloys which tend to adsorb gas when in a liquid state [21]. The gases that are absorbed by the surface are able to diffuse into the metal on an atomic scale. Hydrogen appears as the only gas that can be dissolved in aluminum and its alloys. The small atomic volume makes hydrogen able to diffuse faster into the liquid metal than other gases [35].

One of the methods to reduce the residual stress from welding is to use the vibration welding method. Research on residual stress is very important because residual stress will cause the material to become hard but brittle so it can cause weld structure failures such as brittle fracture, fatigue, and cracking. The vibration method is able to release residual stresses without changing the shape and microstructure [36]. The vibration method is able to reduce residual stresses and is effective for homogenization of concentrated residual stress [14], [15]. Therefore, this article review provides an understanding of how to increase fatigue resistance by reducing porosity and residual stress with the vibration method, so that it will help and facilitate further research.

2. Methods

This study uses a qualitative method through a literature study on vibration welding in aluminum alloy welding. Searching related articles about vibration welding using the scienceDirect database for the last 14 years, from 2008 to August 2022, found as many as 73 articles.

The article search is done by optimizing the Boolean Operator. With keywords "vibration welding" AND "aluminum alloy" found 25 research articles, with keywords "vibration welding" AND "residual stress" found 10 review articles and 18 research articles, and with keywords "vibration welding" AND "porosity " found 20 research articles. From 2015 to the end of 2020, research on vibration welding in aluminum alloy welding and its effect on residual stresses has an increasing trend and has become an interesting study, as presented in **Figure 1**.

A total of 73 articles on vibration welding consist of several types of topics which include; the welding specifications selected, the magnitude of the force and the frequency of vibration used, the type of material to be joined and the mechanical properties tested. Of the 73 articles identified, then screening was carried out and 42 articles were eligible. Of the 42 eligible articles, there are only 12 specific and systematic articles outlining the cause-and-effect series and how to reduce the porosity and residual stress of the aluminum alloy welding joint (**Figure 2**).

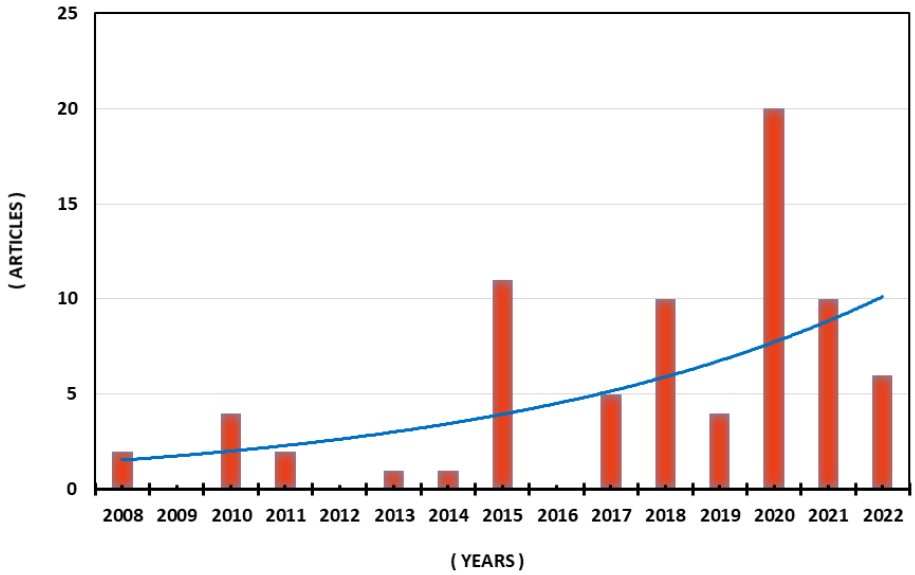

Figure 1. Tend in published work on vibration welding of aluminum alloys

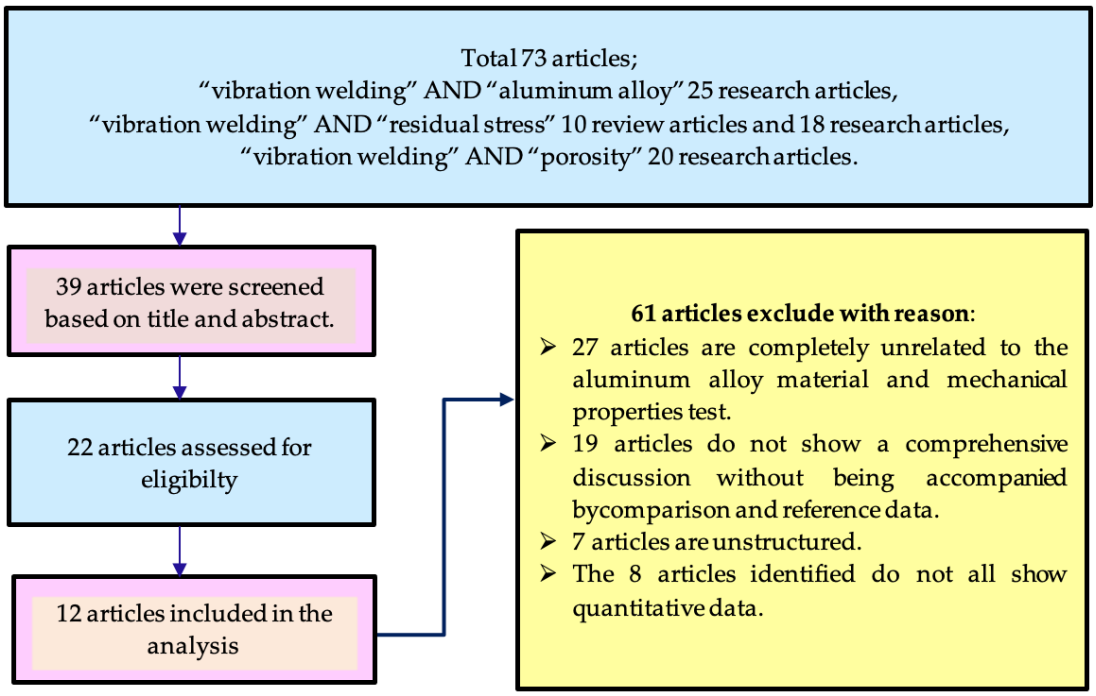

Figure 2. PRISMA diagram of retrieved studies

In the construction of vehicles and transportation equipment, many production technologies are used in each process. One of them is the welding technology used for the connection process between component parts. There are several welding techniques commonly used in the manufacturing industry, such as gas tungsten arc welding (GTAW), gas metal arc welding (GMAW), and flux cored arc welding (FCAW). GMAW welding techniques are most widely used in the maritime, automotive, bridge, and building construction industries. This review article shows further research opportunities related to vibration welding to reduce porosity and residual stress in aluminum alloy welding in the future.

3. Results and Discussion

The results of screening research articles on welding vibration to reduce porosity and residual stress in aluminum alloys are presented in a summary form in **Table 1**.

3.1. Grain Size Refinement

AA5083 welding using GMAW welding with vibration can reduce grain size [37]. By increasing the vibration force of the GMAW welding, it can produce an increase in tensile strength accompanied by an increase in the ductility of the AA5083 welded joint [38]. Providing ultrasonic vibrations at the weld at different joint points between 780 steel and Al 6061 aluminum alloy can increase the strength of the welded joint [39]. Welding due to vibration on aluminum alloy Al 5052 can reduce the grain size in the region and increase the homogeneity of particle distribution [40]. The strength, hardness and ductility of the Friction Stir Vibration (FSV) welded specimen is higher than that of the Friction Stir (FS) welded specimen without vibration [40]. Likewise, the vibration vibrations with a horizontal direction on the Spot Welding are able to produce grain refinement on the welded metal [41].

The microstructure of the weld joint area with ultrasonic vibration is shown in **Figure 3**. The columnar grain size without ultrasonic vibration is larger than with ultrasonic vibration as in **Figure 3a** and **Figure 3c**. While the vibration welding shows the occurrence of columnar grain fragmentation so that the grain size becomes finer as shown in **Figure 3b** and **Figure 3d**.

Table 1. Research articles about vibration welding of aluminum alloy

No	Refs.	Material	Method	Findings	
				Microstructure	Mechanical Properties
1	[42]	6082 Aluminum Alloy	Ultrasonic Vibration Welding (UVW)	The release of residual stress can reduce the value of hardness, thereby increasing ductility.	The residual stress relief rate in one direction is proportional to the vibratory stress introduced in that direction.
2	[39]	6061 Aluminum Alloy and 780 Steel	Ultrasonic Vibration on Resistance Spot Welding (UVRW)	UVRW with a vibration frequency of 60 Hz can increase the bond strength of Al-Fe.	UVRW can increase strength up to 300%.
3	[43]	5A06 Aluminum Alloy	Laser Vibration Welding	The frequency of 100, 200, 300 Hz will accelerate the growth of new grain cores in the process of solidifying the weld metal.	The porosity of the weld is reduced and the tensile strength is increased.
4	[40]	Al5052 Aluminum Alloy	Vibration Friction Stir Welding (VFSW)	Vibration decreases the grain size in the weld region and increases the homogeneity of particles distribution.	Ductility of VFSW welded specimens are higher than FS welded specimens
5	[44]	AA6061-T6 Aluminum Alloy	Ultrasonic Vibration Friction Stir Welding (UVeFSW)	With UVeFSW, the grain orientation of the weld is more random.	The results of the weld are stronger to withstand dislocations.
6	[19]	AA2024 Aluminum Alloy	Vibration Friction Stir	The application of ultrasonic vibrations makes the particle phase smaller, the number of particles is	VFSW contributes to increased fatigue resistance.

No	Refs.	Material	Method	Findings	
				Microstructure	Mechanical Properties
			Welding (VFSW)	greater and the distribution of the particles is more uniform.	
7	[45]	6061-T4 Aluminum Alloy and Mg-AZ31B	Ultrasonic Vibration Friction Stir Welding (UVeFSW)	Ultrasonic vibration causes a reduction in the thickness of the weld layer, but does not change the chemical composition of the compound layer formed Al_3Mg_2.	Vibration will increase the mechanical interlocking of the Al-Mg alloy so that the weld strength increases
8	[38]	AA5083 Aluminum Alloy	Vibration Gas Metal Arc Welding (VGMAW)	There was a grain size refinement from 140 m to 130 m, and 115 m at each of 400 N, 750 N, 1000 N vibrations.	Elongation increased 6%, 9%, and 16.5% for each of the 400 N, 750 N and 1000 N vibration force variables.
9	[46]	AA5083 Aluminum Alloy	Vibration Metal Inert Gas (VMIG)	At the application of 300 Hz vibration, it is able to increase the tensile strength by about 51.3% due to grain refinement and the increase in the number of equiaxed dendritic microstructures in the weld metal area, resulting in the best fatigue crack propagation resistance.	The hardness of the weld metal and HAZ increases due to the increasing number of dislocations which will result in strain hardening. It is also affected by the residual stress (compression) in both parts.
10	[47]	AA5083 Aluminum Alloy	Vibration Metal Inert Gas (VMIG)	The microstructure becomes smoother and homogeneity occurs at the weld joint.	Increasing the vibration power between 0–200 W will decrease the porosity.
11	[48]	AA1050 Aluminum Alloy and C1100 copper alloy	Ultrasonic Vibration Welding (UVW)	non-directional planar vibration is able to produce welding strength up to 1.7% compared to using linear vibration direction.	This planar vibration will cause joint interface vibration.
12	[49]	7A52 Aluminum Alloy	Vibration Gas Metal Arc Welding (VGMAW)	Vibration frequency of 19.5 kHz can reduce grain size from 151.3 μm to 08.6 μm.	The fracture strength increased from 305.9 MPa to 342 MPa, and the elongation increased from 5.4% to 7.4%.

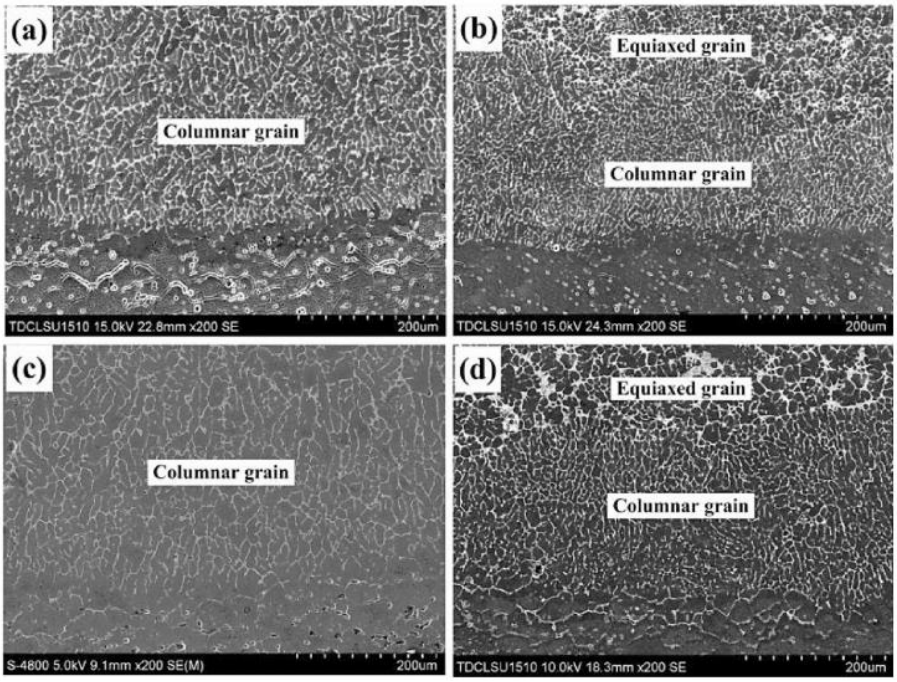

Figure 3. SEM area of two welded joints: (a and c) Non-ultrasonic vibration; (b and d) ultrasonic vibrations [50]

The application of vibration can cause the movement of dendritic grains to come into contact with the cold liquid in the weld pool which will result in a higher cooling rate. An increase in the cooling rate, will result in grain refinement [41]. In addition, vibration can cause cavitation and bubble collapse resulting in increased nucleation [51], [52]. The mechanism of grain refinement due to cavitation can be explained as follows: (1), Under cavitation, the collapse of the bubble causes an increase in negative pressure. According to [52] that the melting temperature under these conditions increases, which will result in an increase in undercooling and an increase in nucleation. The increase in melting temperature, according to [50], [53] follows Equation (1).

$$^{\triangle}T_m = T_m{}^{\triangle}P{}^{\triangle}V/{}^{\triangle}H \quad (1)$$

Where T_m, P, V, and H are the melting temperature, pressure change, volume change, and enthalpy change. (2), According to [54] that columnar grains will crack and break due to cavitation, which promotes heterogeneous nucleation resulting in grain refinement [51]. These columnar grain fractions will form fine equiaxed grains. From research [55] stated that cavitation enhances inclusions as an effective nucleation site to generate active nuclei.

Figure 4a and **Figure 4b** describe the results of scanning electron microscope (SEM) surface morphology of the FSW junction fracture without vibration [56]. The fault shows the characteristics of a flat and slightly dimple surface with small size [57], [58]. While the surface morphology of the ultrasonic vibration assisted-friction stir welding (UVaFSW) joint fracture with a vibration frequency of 20 kHz and a vibration amplitude of 25 μm shows the characteristics of a wider and more numerous dimple surface as shown in **Figure 4c** and **Figure 4d**. The fracture surface features show a ductile mode fracture. This is due to the presence of very fine recrystallized grains due to plastic deformation in the heat affect zone (HAZ) region [59].

FSW involves complex interactions between various simultaneous thermomechanical processes. The interaction will affect heating and cooling rates, plastic deformation and flow, dynamic recrystallization, and mechanical joints. Heat Affected Zone (HAZ), is the area closest to the welding location, the material in this area experiences a thermal cycle which causes changes in the microstructure and mechanical properties of the base metal.

Recent studies have shown that MIG welding with a vibration frequency of 300 Hz on aluminum AA5083 series is able to reduce the rate of fatigue crack growth resistance in the weld area [46]. The finer-grained microstructure will provide more grain boundaries. This grain boundary can act as an inhibitor for fatigued cracks to propagate. In addition, an equiaxed den-

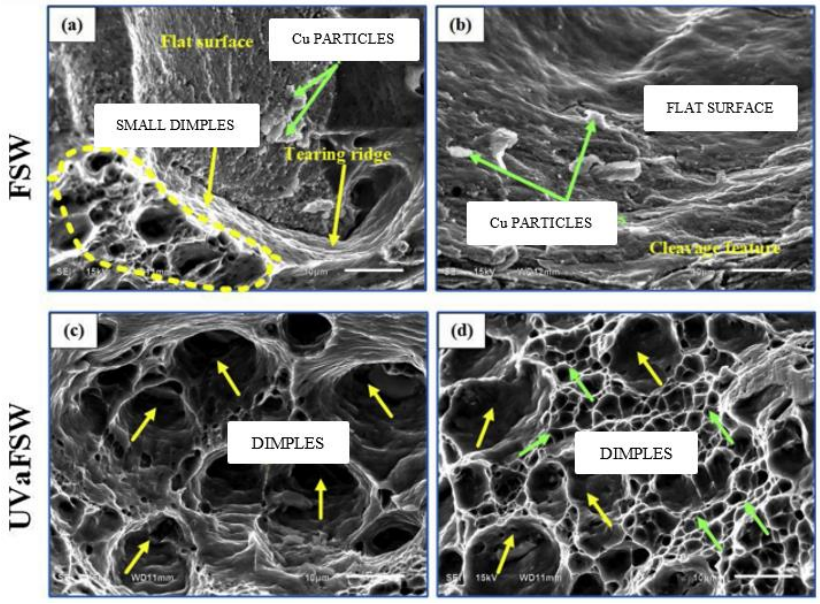

Figure 4. Fracture surface morphologies for FSW (a and b) and UVaFSW; frequency 20 kHz and amplitude 25 μm (c and d) joints prepared at 600 rev/min and 20 mm/min [56]

dritic structure with radially oriented arms results in an 'interlocking structure' that can inhibit fatigue crack propagation.

The results of grain measurements on spot-welded tungsten arc (GTA) gas using the American Society for Testing and Materials (ASTM) E112-13 standard by calculating the average ratio between grain length and grain width are described in **Figure 5**. **Figure 5a** shows the grain size base material (BM), and **Figure 5b** illustrates the reduction in grain size with increasing ultrasonic vibration (USV) time. The increase in USV time to 6 seconds can reduce grain size by up to 48% compared to welded without USV.

3.2. *Increased Hardness And Precipitation Homogenization*

The average hardness values of welded joints with vibration is higher than that of welded joints without vibration [50], [60]. The increase in the hardness value was due to grain size refinement [61]. The average crystallite size of the fusion zone (FZ) decreases with vibration treatment, Which contributes to the increases in microhardness. However, the vibration has no effect on the microstructure of the heat effect zone (HAZ), as shown in **Figure 6**.

The application of FSW ultrasonic vibration to AA2024 aluminum alloy welding resulted in an increase in fatigue resistance [19], due to an even and uniform grain distribution [56]. **Figure 7** shows the fusion zone (FZ) precipitation phase distribution of Mg alloy welds welded with and without ultrasonic vibration-assisted (UVA) treatment [62]. The depositional phase of $Mg_{17}Al_{12}$ occurs during the TIG welding process without vibration as shown in **Figure 7a**. As a brittle phase [63], $Mg_{17}Al_{12}$ will reduce the strength of the weld joint. However, with vibration treatment, the $Mg_{17}Al_{12}$ precipitation phase was evenly distributed throughout the welding FZ due to the cavitation effect [64], [65], as shown in **Figure 7b**.

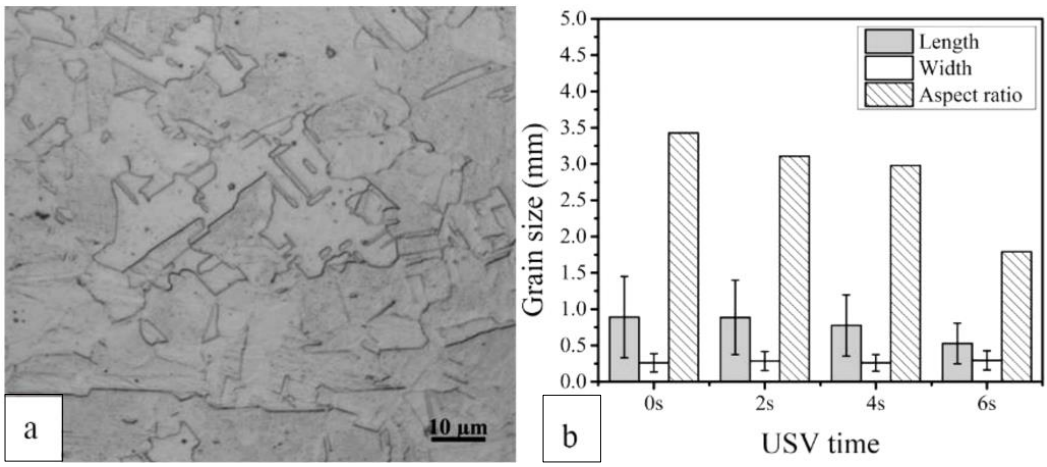

Figure 5. (a) The microstructure of the BM; and (b) the grain size and aspect ratio for GTA spot-welded copper joints with different USV times [66]

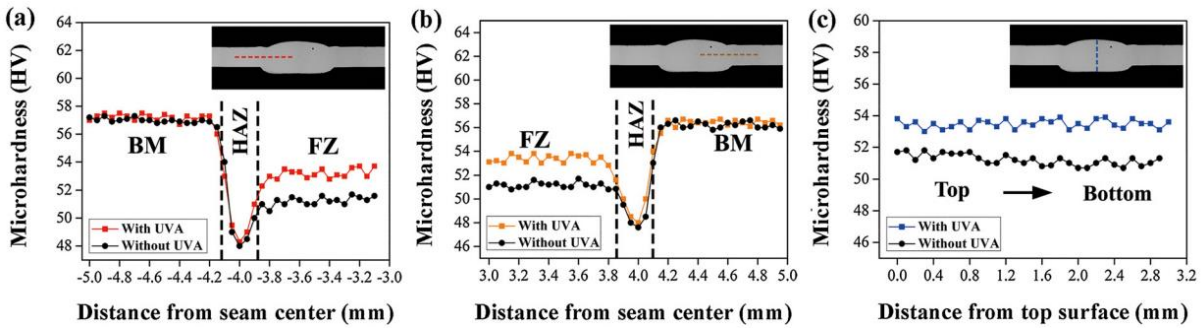

Figure 6. Typical microshardness distribution of AZ31/MB3 Mg alloy joint with welding current of 90A and vibration power of 1.0 kW: (a) and (b) MB3 side and AZ31 side of joint along the horizontal direction, (c) along the vertical direction [62]

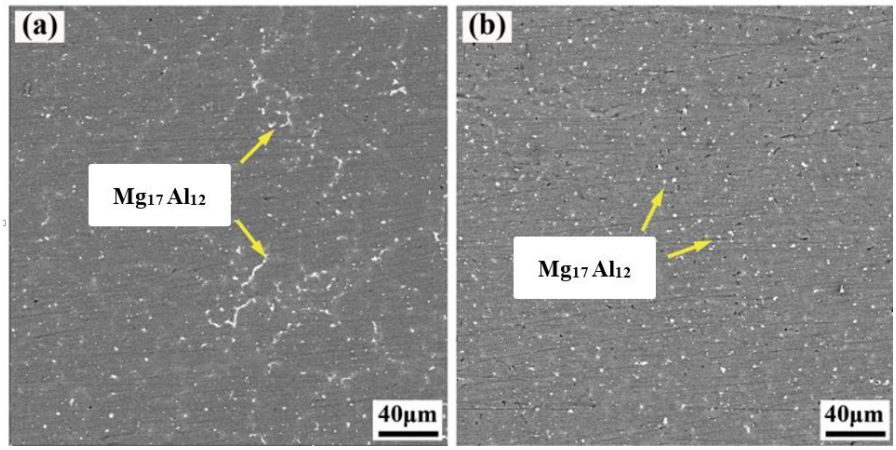

Figure 7. Typical microstructures of FZ of Mg alloy weldments welded with current of 90A: (a) without vibration treatment, (b) with vibration power of 1.0 kW) [62]

3.3. *Reduction of Porosity*

Figure 8 shows the percentage of porosity area in the welded and unaided cross-section of the USV [66]. Vibration welding is able to reduce porosity [47] because of the movement and movement of gas from the bottom to the surface of the weld pool during the compaction process [67]. Vibration will cause internal pressure on the molten weld metal so that trapped gas bubbles float on the surface of the welding pool and come out [50]. Vibration welding can reduce porosity due to an increase in heat dissipation. With vibration it will increase the internal pressure, so that trapped hydrogen bubbles will move up to the surface of the molten metal and escape [66].

According to [66], the internal pressure that occurs (Pa) on the molten weld metal due to ultrasonic vibrations so that bubbles rise to the surface of the molten metal is expressed by Equation (2).

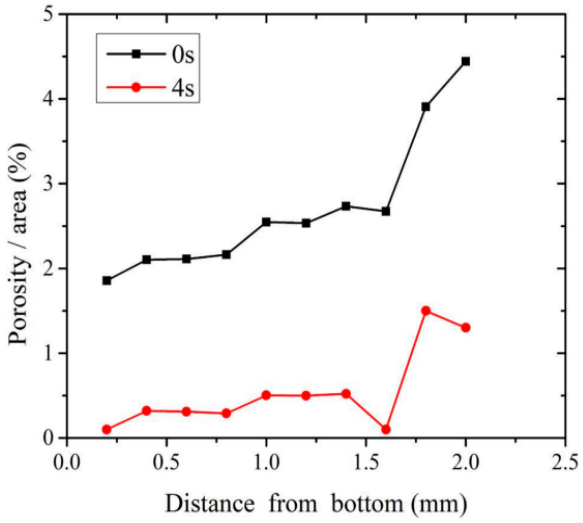

Figure 8. The distribution of porosity from bottom to top surfaces in GTA spot-welded joints with and without vibration assistance [66]

$$Pa = \sqrt{\frac{2Nac\rho_o C_o}{S}} \quad (2)$$

Where Pa is the acoustic intensity; Nac is the output power of the ultrasonic device; ρ_o is the density of the workpiece material being welded, C_o is the ultrasound velocity in the melt of the workpiece material; and S is the area of the ultrasonic projection on the molten metal represented by the curvature contact surface of the weld pool with the HAZ. The surface area of the projection plane (S) is expressed by Equation (3).

$$S = 2\pi\int_{-1}^{1}\sqrt{1+(\frac{dy}{dx})^2}\,dx \quad (3)$$

The reduction in porosity is also evident at the GTA-USV connection as shown in **Figure 9c** and **Figure 9d**. With vibration, the microporosity in the nugget zone (NZ) area due to H_2O vapor bubbles is reduced with a structure in the form of fine equiaxid dendrites. Meanwhile, **Figure 9a** and **Figure 9b** shows the microstructure of GTA welded joints without USV with larger grain sizes and more microporosity [68]. The semi-melt area (fusion line) connecting the HAZ and NZ for the connection without USV is also approximately 100–200 μm wider. This is also confirmed by the SEM results of surface fractures in the fusion line and NZ regions as shown in **Figure 10**.

The large number of small pores will cause the gas to gather to form a larger porosity. Pores grow

in supersaturated liquids by diffusion of gases from liquid to bubbles [69]. The rate of diffusion depends on the surface energy of the bubbles and the pressure of the molten metal. When the bubble moves to the surface of the molten metal, the pressure is reduced. The growing bubbles cause the diffusion of the liquid metal gas atoms towards the bubbles [70]. The increase in pore size provides additional opportunities for bubbles to move to the surface of the molten metal.

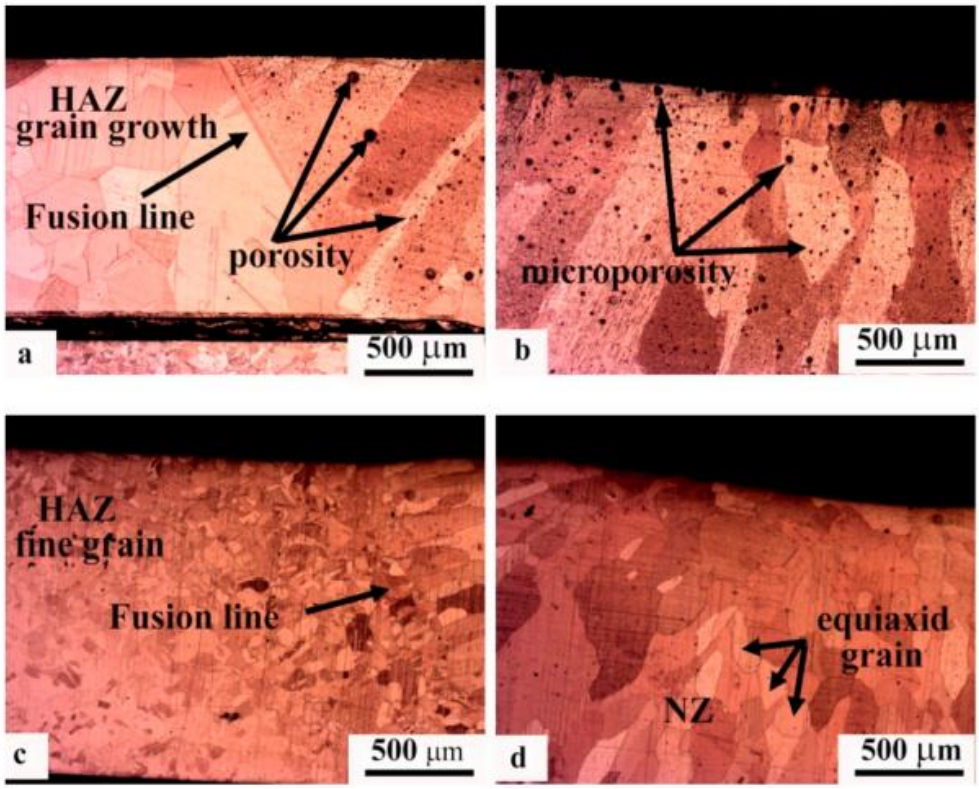

Figure 9. The cross-section microstructure of GTA spot-welded joints. (a,b) welded without USV; and (c,d) welded with USV assistance [66]

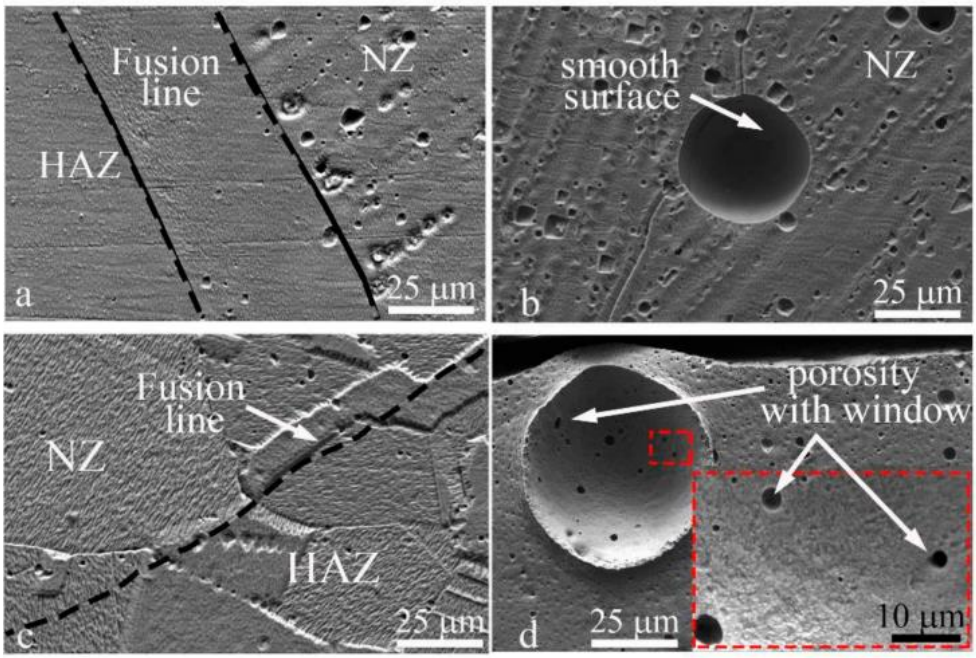

Figure 10. SEM images of porosity at the NZ of a GTA spot-welded copper joint made without USV (a) at the fusion line; (b) at the center of NZ; and with USV; (c) at fusion line; and (d) at the center of NZ [66]

3.4. Improved Mechanical Strength

GMA welding on similar joints of aluminum alloy series AA5083 with vibration frequencies of 50 Hz, 75 Hz and 90 Hz, respectively, resulted in a significant reduction in grain size during the application of vibration during welding [37]. GMAW welding, the AA5083 series aluminum alloy similar connection by increasing the vibration force from 400 N to 750 N and 1000 N is able to increase the tensile stress by about 3% and the elongation also increases from 6% to 9% and 16.5% [38]. Vibration method welding on similar material AA5083 with a vibration frequency of 300 Hz and a vibration amplitude of 5 μm is able to increase the tensile strength by about 51.3% due to grain size refinement [26], [46]. The result of tensile tests is shown in **Figure 11**. The GMA welded joint showed the lower tensile strength (305.9 MPa), yield strength (277.6 MPa) and elongation (5.4%). Therefore, the UTS, yield strength, and elongation of the V-GMA welded joint are 13%, 7%, and 37%, respectively, higher than those of the GMA welded joint [49].

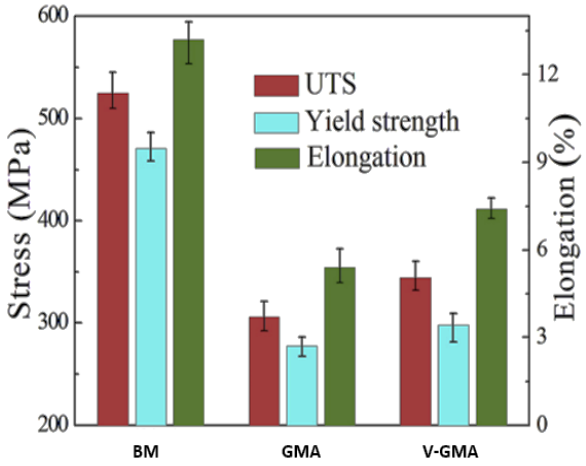

Figure 11. Tensile strength and elongation of the welded samples, base metal (BM), gas metal arc (GMA), Vibration gas metal arc (V-GMA) [49]

The smaller the size of the metal, the greater the strength. This is in accordance with equation (4) Hall-Petch [71].

$$\sigma_y = \sigma_0 + k_y . d^{-1/2} \quad (4)$$

With, σ_y = yield strength, σ_0 = shear stress in the opposite direction to the movement of dislocations in the grain, k_y = material constant representing the degree of difficulty to produce grain dislocation, and d = grain diameter.

3.5. Acceleration of Nuleates Growth

The natural frequency of the vibration generating system can be calculated using equation (5).

$$\omega_n = \sqrt{\frac{k}{m}} \text{ (rad/s)} \quad \text{or} \quad f_n = \frac{1}{2\pi}\sqrt{\frac{k}{m}} \text{ (Hz)} \quad (5)$$

Where, k = spring constant and m = mass (Kg). From equation (5) it is known that the natural frequency depends on the stiffness and weight of a vibrating system. If the magnitude of the vibration frequency that arises is equal to the natural frequency possessed by the system, it will cause resonance in the system [46].

The effect of vibration on the acceleration of new grain growth and dendrite morphology can be illustrated as shown in **Figure 12**. By applying vibration in both horizontal and vertical directions, it will result in an increase in the cooling rate (fast cooling rate) and an increase in the temperature gradient (high temperature gradient), so that it will accelerate growth of nucleates in the middle molten metal [41].

By giving vibration to the molten weld metal, the secondary dendritic branch or arm will break and form a new solid phase core which will then grow into grains. The more grains, the more random the grain orientation of the weld will be [44]. And the strength of the weld metal will increase because the grain boundaries are dislocation inhibitors [71].

The application of vibration during welding is also able to significantly reduce the peak temperature of the HAZ due to rapid cooling [66] as shown in **Figure 13a**. The peak temperature in the HAZ reaches 565 °C when welding without USV. The duration of temperature above 100 °C when welding with USV is around 100 second, much shorter than the process without USV connection of 200 second. The cooling rate increases with increasing USV time as shown in **Figure 13b**. Vibration with an ultrasonic frequency of 28 kHz increases the rate of heat dissipation from the weld joint. Increasing the rate of heat dissipation (cooling rate) will reduce grain growth in the HAZ so that it will form equiaxed grains during NZ compaction.

3.6. Reduction of Residual Stress

Residual stress measurements were carried out using the neutron diffraction method using the

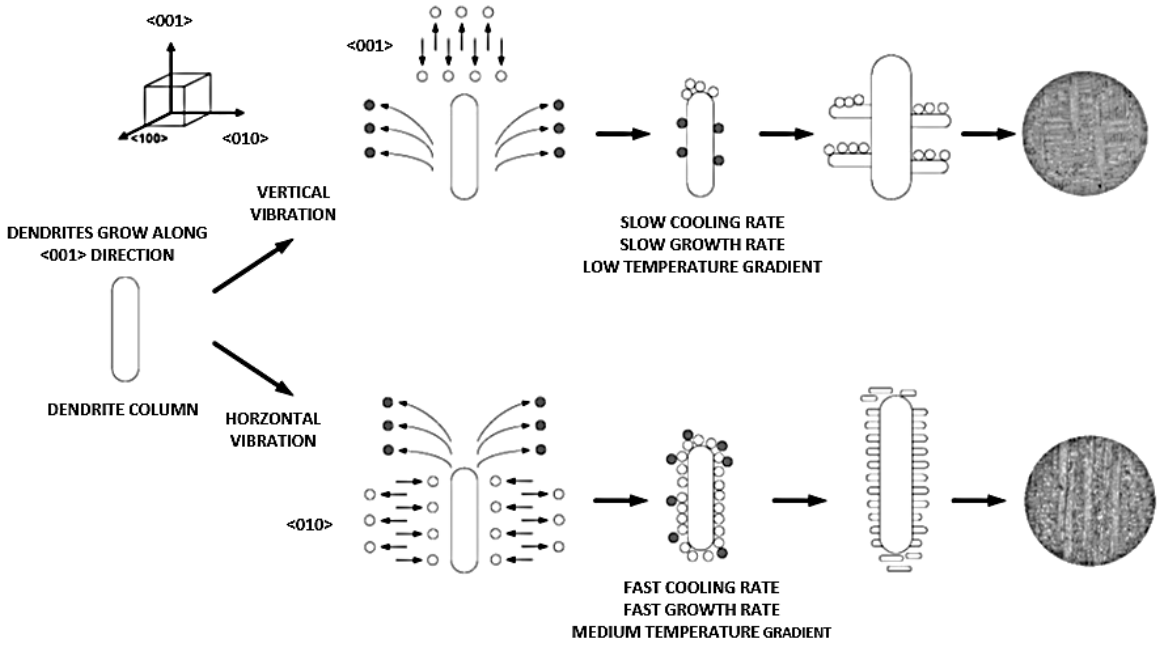

Figure 12. Illustration of effects of vibration on dendrite morphologies; ●=nucleates from convection, o=nucleates from vibration [41]

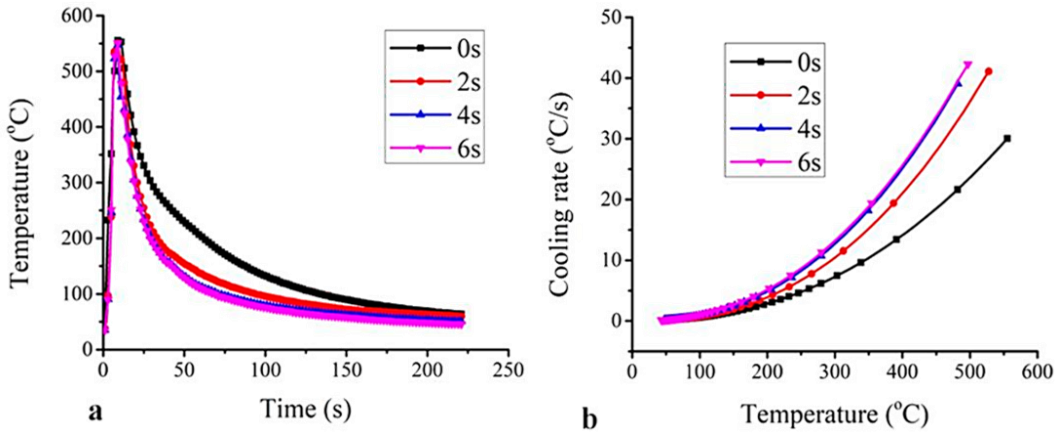

Figure 13. (a) The heating and cooling history of welded joints with and without USV; (b) the cooling rate vs. temperature of welded joints [66]

DN1-M Neutron Diffractometer. The neutron beam that enters through the monochromator is directed to the test object with an angle θ. The neutron beam will be reflected symmetrically with an angle θ then captured by the monitor detector. Specimen measurements were carried out in the normal, transverse and longitudinal directions. The wavelength of the neutron (λ) is determined from the results of the basic material test. From the profile graph of the diffraction results, the value of the peak angle (θ) will be obtained which will then be used to calculate the lattice distance (d) using the Equation (6).

$$d = \frac{\lambda}{2\sin\theta} \quad (6)$$

So the amount of strain (ε) can be determined by the Equation (7).

$$\varepsilon = \frac{d - d_0}{d_0} \quad (7)$$

d_0 is measured at a stress-free point (that is far from the weld point). The amount of stress (σ) can be calculated using the Equation (8).

$$\sigma = [E/(1-2\nu)]\ \varepsilon_{av} \quad (8)$$

with, E the elastic modulus, ν poison ratio and εav the average stress.

The vibration method is able to reduce residual stresses and is effective for homogenization of concentrated residual stress [42]. The vibration

method is able to release residual stresses [50] without changing the shape and microstructure [36]. MIG welding with a vibration frequency of 300 Hz is able to reduce the longitudinal residual stress in the weld area from 193 MPa without vibration to 107.8 MPa and is able to reduce the transverse residual stress in the HAZ from 125.5 MPa to 75.0 MPa [46] as in **Figure 14**.

The ultrasonic vibratory stress relief (UVSR) method with 20 kHz on AA6082 was able to reduce residual stress up to 53%, and was effective for homogenization of concentrated residual stress up to 57% (from the initial distribution interval of 40-110 Mpa to 30-60 Mpa) [42]. Reduction of residual stress in the transverse direction as shown in **Figure 15a** and the longitudinal direction as shown in **Figure 15b**. Referring to **Figure 15a** the transverse residual stresses at point 8 and the longitudinal residual stresses at points 5 and 4, the initial residual stresses are 110 MPa, 90 MPa and 100 MPa. With the application of vibration there is a reduction in stress at that point to 25 MPa, 25 MPa and 20 MPa, respectively. The ratio of residual stress reduction that occurs is 77%, 72% and 80%.

Vibration contributes to the formation of dislocations [14], [15]. The movement of the dislocations will result in the initial residual stress resulting in several new dislocations [72]. The evolution of this dislocation will produce two residual stress changes in the form of: residual stress reduction and residual stress homogenization [58], [73]. The magnitude of the transverse residual stress is relatively lower than the longitudinal residual stress. This is because the expansion and contraction/shrinkage during welding along the transverse direction, i.e. perpendicular to the weld line is lower than the longitudinal direction [74].

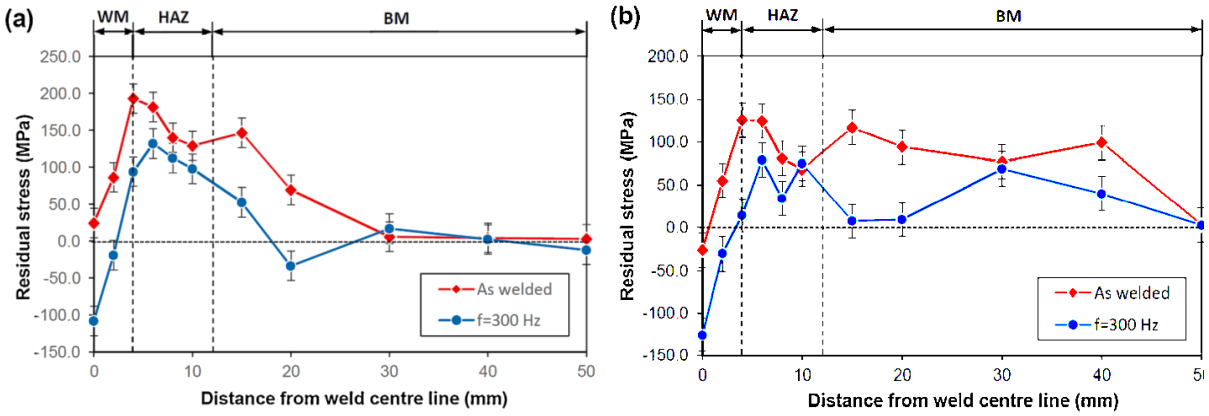

Figure 14. (a) Longitudinal residual stress; (b) transverse residual stress profiles for the welded joints in as welded condition and vibrational treatment at 300 Hz. Notes: WM is weld metal, HAZ is heat affected zone and BM is base metal [46]

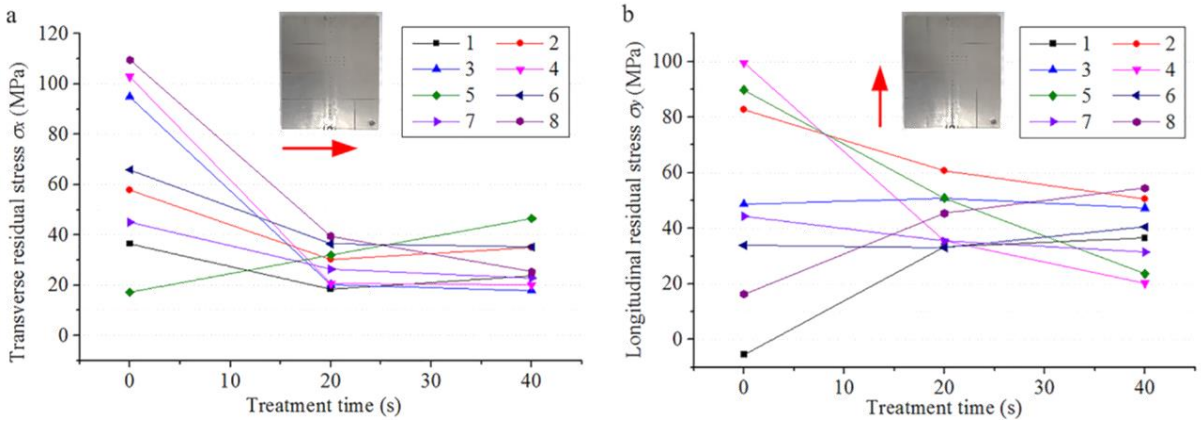

Figure 15. The transverse and longitudinal residual stress changes along UVSR treatment time: (a) transverse residual stress σx; (b) longitudinal residual stress σy [42]

4. Conclusion

From the literature review on vibration welding in aluminum alloy welding, it can be concluded that the choice of vertical or horizontal vibration direction must be adjusted to the type of welding. The determination of the magnitude of the vibration frequency should not approach the natural frequency of the vibrating system because it will produce a resonance with a very high amplitude. Vibration perpendicular to the direction of dendritic growth will result in better grain refinement. This vibration will promote the dendrites to come into contact with the cold liquid and make the dendrites cool faster so that the growth of new nuclei will also increase. The finer the grain size of the equiaxed dendrites produced, the more grain boundaries as dislocation inhibitors, so it will increase the mechanical strength. The vibration method also causes a cavitation effect so that precipitation as a brittle phase will be evenly distributed throughout the welding FZ. The dendritic structure is equiaxed with radially oriented arms due to vibration resulting in an 'interlocking structure' which can inhibit fatigue crack propagation. By giving vibration during welding, in addition to heat dissipation which will accelerate the cooling rate, it also causes internal pressure on the molten weld metal. This internal pressure will push the air bubbles trapped in the molten metal up to the surface and leave the weld metal which will reduce the porosity of the weld. Increasing the cooling speed will reduce the HAZ area and reduce the temperature gradient so as to reduce residual stress due to temperature differences during the welding process.

5. Scope for Further Work

Previous studies on vibration welding have only discussed the effect of vibration on; mechanical characteristics, joint strength, microstructure, and grain size, but not much has been discussed specifically their effect on reducing porosity and fatigue crack propagation rate in welding aluminum alloy dissimilar materials. Therefore, it is necessary to conduct further research to determine the effect of varying the frequency of vibration on welding aluminum alloy dissimilar materials to; porosity and fatigue crack propagation rate due to residual stress caused by different heating and cooling rates.

Acknowledgements

The authors are grateful to the Ministry of Education, Culture, Research, and Technology of the Republic of Indonesia for funding this research through a PDD grant scheme, with Research Contract No. 096/E5/PG.02.00.PT/2022.

Author's Declaration

Authors' contributions and responsibilities

Conceptualization: Saifudin; Resources: Saifudin, Nurul Muhayat, Eko Surojo, Yupiter HP Manurung, Triyono; Writing-original draft preparation: Saifudin, Nurul Muhayat, Eko Surojo, Yupiter HP Manurung, Triyono; Writing-review and editing: Saifudin, Nurul Muhayat, Eko Surojo, Yupiter HP Manurung, Triyono. All authors have read and agreed to the published version of the manuscript.

Funding

Ministry of Education, Culture, Research, and Technology of the Republic of Indonesia.

Availability of data and materials

All data are available from the authors.

Competing interests

The authors declare no competing interest.

Additional information

No additional information from the authors.

References

[1] R. P. Putra, D. Yuvenda, M. Setiyo, A. Andrizal, and M. Martias, "Body City Car Design of Two Passengers Capacity: A Numerical Simulation Study," *Automotive Experiences*, vol. 5, no. 2, pp. 163–172, 2022.

[2] Z. Arifin *et al.*, "Aerodynamic Characteristics of Ahmed Body with Inverted Airfoil Eppler 423 and Gurney Flap on Fastback Car," *Automotive Experiences*, vol. 5, no. 3, pp. 355–370, 2022.

[3] G. Refiadi, I. S. Aisyah, and J. P. Siregar, "Trends in lightweight automotive materials for improving fuel efficiency and reducing carbon emissions," *Automotive Experiences*, vol. 2, no. 3, pp. 78–90, 2019, doi: 10.31603/ae.v2i3.2984.

[4] R. Widyorini, N. H. Sari, M. Setiyo, and G. Refiadi, "The Role of Composites for Sustainable Society and Industry," *Mechanical Engineering for Society and Industry*, vol. 1, no. 2, pp. 48–53, 2021.

[5] L. B. Godefroid, G. L. de Faria, L. C. Cândido, and S. C. Araujo, "Fatigue failure of a welded

automotive component," *Procedia materials science*, vol. 3, pp. 1902–1907, 2014.

[6] K. Shrama, "Fatigue of welded high strength steels for automotive chassis and suspension applications." Cardiff University, 2016.

[7] S. Suntari, H. Purwanto, S. M. B. Respati, S. Sugiarto, and Z. Abidin, "Effect of Electrode Diameter and Current on Dissimilar Metal Welding (Stainless Steel-Galvanized Steel) in Bus Body Construction: Microstructure and Properties Evaluation," *Automotive Experiences*, vol. 5, no. 3, pp. 402–415, 2022.

[8] N. Muhayat, Y. A. Matien, H. Sukanto, and Y. C. N. Saputro, "Fatigue life of underwater wet welded low carbon steel SS400," *Heliyon*, vol. 6, no. 2, p. e03366, 2020.

[9] Y. Zhao, X. Zhou, T. Liu, Y. Kang, and X. Zhan, "Investigate on the porosity morphology and formation mechanism in laser-MIG hybrid welded joint for 5A06 aluminum alloy with Y-shaped groove," *Journal of Manufacturing Processes*, vol. 57, no. July, pp. 847–856, 2020, doi: 10.1016/j.jmapro.2020.07.044.

[10] M. N. Ilman and R. Soekrisno, "Corrosion fatigue behavior of resistance spot welded dissimilar metal welds between carbon steel and austenitic stainless steel with different thickness," *Procedia Engineering*, vol. 10, pp. 649–654, 2011.

[11] S. Tathgir, D. W. Rathod, and A. Batish, "Emphasis of Weld Time, Shielding Gas and Oxygen Content in Activated Fluxes on the Weldment Microstructure," *Mechanical Engineering for Society and Industry*, vol. 1, no. 2, pp. 86–95, 2021, doi: 10.31603/mesi.5903.

[12] M. W. Tjaronge, V. Sampebulu, and R. Djamaluddin, "Porosity and Microstructure Phase of Self Compacting Concrete Using Sea Water as Mixing Water and Curing," in *Advanced Materials Research*, 2015, vol. 1119, pp. 647–651.

[13] R. D. Ardika, T. Triyono, and N. Muhayat, "A review porosity in aluminum welding," *Procedia Structural Integrity*, vol. 33, pp. 171–180, 2021.

[14] L. Pan *et al.*, "Welding residual stress impact on fatigue life of a welded structure," *Welding in the World*, vol. 57, no. 5, pp. 685–691, 2013.

[15] H. Gao, Y. Zhang, Q. Wu, J. Song, and K. Wen, "Fatigue life of 7075-T651 aluminium alloy treated with vibratory stress relief," *International Journal of Fatigue*, vol. 108, pp. 62–67, 2018.

[16] Q. Jin *et al.*, "A primary plus secondary local PWHT method for mitigating weld residual stresses in pressure vessels," *International Journal of Pressure Vessels and Piping*, vol. 192, p. 104431, 2021.

[17] E. D. W. S. Putri, E. Surojo, and E. P. Budiana, "Current research and recommended development on fatigue behavior of underwater welded steel," *Procedia Structural Integrity*, vol. 27, pp. 54–61, 2020.

[18] Z. Gao, B. Gong, Y. Liu, D. Wang, C. Deng, and D. Hu, "Fatigue-performance of PWHT welded joints: As-welded vs. high-frequency mechanical impact treatment," *Journal of Constructional Steel Research*, vol. 187, p. 106933, 2021.

[19] M. Wu, C. Wu, and S. Gao, "Effect of ultrasonic vibration on fatigue performance of AA 2024-T3 friction stir weld joints," *Journal of Manufacturing Processes*, vol. 29, pp. 85–95, 2017.

[20] X. Liang, Y. Wan, C. Zhang, B. Zhang, and X. Meng, "Comprehensive evaluation of welding quality for butt-welded by means of CO2 arc vibratory welding," *The International Journal of Advanced Manufacturing Technology*, vol. 90, no. 5, pp. 1911–1920, 2017.

[21] K. P. Mehta, "A review on friction-based joining of dissimilar aluminum – steel joints," *Early career scholars in materials sciensce*, 2019, doi: 10.1557/jmr.2018.332.

[22] W. Liu, H.-P. Wang, F. Lu, H. Cui, and X. Tang, "Investigation on effects of process parameters on porosity in dissimilar Al alloy lap fillet welds," *The International Journal of Advanced Manufacturing Technology*, vol. 81, no. 5, pp. 843–849, 2015.

[23] M. Samiuddin, J. Li, M. Taimoor, M. N. Siddiqui, S. U. Siddiqui, and J. Xiong, "Investigation on the process parameters of TIG-welded aluminum alloy through mechanical and microstructural characterization," *Defence Technology*, vol. 17, no. 4, pp. 1234–1248, 2021.

[24] S. C. Wu, C. Yu, W. H. Zhang, Y. N. Fu, and L. Helfen, "Porosity induced fatigue damage of laser welded 7075-T6 joints investigated via synchrotron X-ray microtomography,"

Science and Technology of Welding and Joining, vol. 20, no. 1, pp. 11–19, 2015.

[25] R. Lin, H. Wang, F. Lu, J. Solomon, and B. E. Carlson, "Numerical study of keyhole dynamics and keyhole-induced porosity formation in remote laser welding of Al alloys," *International Journal of Heat and Mass Transfer*, vol. 108, pp. 244–256, 2017.

[26] I. Khoirofik, "Analisa Teknis Pengelasan Dissimilar Material Antara Aa 6063 Dan Aa 5083 Ditinjau Dari Aspek Mekanik Dan Metalurgi Pada Bangunan Kapal," Institut Teknologi Sepuluh November, 2015.

[27] X. Zhan, Y. Zhao, Z. Liu, Q. Gao, and H. Bu, "Microstructure and porosity characteristics of 5A06 aluminum alloy joints using laser-MIG hybrid welding," *Journal of Manufacturing Processes*, vol. 35, no. August, pp. 437–445, 2018, doi: 10.1016/j.jmapro.2018.08.011.

[28] S. Sivabalan, R. Sridhar, A. Parthiban, and G. Sathiskumar, "Experimental investigations of mechanical behavior of friction stir welding on aluminium alloy 6063," *Materials Today: Proceedings*, no. xxxx, 2020, doi: 10.1016/j.matpr.2020.07.236.

[29] Y. Murakami, "Influence of Si-phase on fatigue properties of aluminium alloys," *Metal Fatigue*, pp. 269–291, 2019, doi: 10.1016/b978-0-12-813876-2.00012-1.

[30] L. Chen, C. Wang, L. Xiong, X. Zhang, and G. Mi, "Microstructural, porosity and mechanical properties of lap joint laser welding for 5182 and 6061 dissimilar aluminum alloys under different place configurations," *Materials and Design*, vol. 191, p. 108625, 2020, doi: 10.1016/j.matdes.2020.108625.

[31] W. Zheng, Y. He, J. Yang, and Z. Gao, "Hydrogen diffusion mechanism of the single-pass welded joint in welding considering the phase transformation effects," *Journal of Manufacturing Processes*, vol. 36, pp. 126–137, 2018.

[32] M. Brůna and A. Sládek, "Hydrogen analysis and effect of filtration on final quality of castings from aluminium alloy AlSi7Mg0. 3," *Archives of Foundry Engineering*, vol. 11, no. 1, pp. 5–10, 2011.

[33] L. Huang, X. Hua, D. Wu, L. Fang, Y. Cai, and Y. Ye, "Effect of magnesium content on keyhole-induced porosity formation and distribution in aluminum alloys laser welding," *Journal of Manufacturing Processes*, vol. 33, no. January, pp. 43–53, 2018, doi: 10.1016/j.jmapro.2018.04.023.

[34] H. Yu, Y. Xu, J. Song, J. Pu, X. Zhao, and G. Yao, "On-line monitor of hydrogen porosity based on arc spectral information in Al–Mg alloy pulsed gas tungsten arc welding," *Optics & Laser Technology*, vol. 70, pp. 30–38, 2015.

[35] X. Han, Z. Yang, Y. Ma, C. Shi, and Z. Xin, "Porosity distribution and mechanical response of laser-MIG hybrid butt welded 6082-T6 aluminum alloy joint," *Optics and Laser Technology*, vol. 132, no. May, p. 106511, 2020, doi: 10.1016/j.optlastec.2020.106511.

[36] M. Burzić, R. Prokić-Cvetković, M. Manjgo, L. Milović, M. Arsić, and O. Popović, "Effect of vibration on the variation of residual stresses and impact energy in butt-welded joints," *Integritet i vek konstrukcija*, vol. 12, no. 3, pp. 215–220, 2012.

[37] R. Tamasgavabari, A. R. Ebrahimi, S. M. Abbasi, and A. R. Yazdipour, "Effect of harmonic vibration during gas metal arc welding of AA-5083 aluminum alloy on the formation and distribution of intermetallic compounds," *Journal of Manufacturing Processes*, vol. 49, pp. 413–422, 2020.

[38] R. Tamasgavabari, A. R. Ebrahimi, S. M. Abbasi, and A. R. Yazdipour, "The effect of harmonic vibration with a frequency below the resonant range on the mechanical properties of AA-5083-H321 aluminum alloy GMAW welded parts," *Materials Science and Engineering: A*, vol. 736, pp. 248–257, 2018.

[39] U. Shah and X. Liu, "Effects of ultrasonic vibration on resistance spot welding of transformation induced plasticity steel 780 to aluminum alloy AA6061," *Materials & Design*, vol. 182, p. 108053, 2019.

[40] S. Fouladi and M. Abbasi, "The effect of friction stir vibration welding process on characteristics of SiO2 incorporated joint," *Journal of Materials Processing Technology*, vol. 243, pp. 23–30, 2017.

[41] C.-W. Kuo, S.-M. Yang, J.-H. Chen, G.-H. Lai, and W. Wu, "Study of vibration welding mechanism," *Science and Technology of Welding and Joining*, vol. 13, no. 4, pp. 357–

362, 2008.

[42] Q. Zhang, L. Yu, X. Shang, and S. Zhao, "Residual stress relief of welded aluminum alloy plate using ultrasonic vibration," *Ultrasonics*, vol. 107, p. 106164, 2020.

[43] Z. Wang, J. P. Oliveira, Z. Zeng, X. Bu, B. Peng, and X. Shao, "Laser beam oscillating welding of 5A06 aluminum alloys: Microstructure, porosity and mechanical properties," *Optics & Laser Technology*, vol. 111, pp. 58–65, 2019.

[44] G. K. Padhy, C. S. Wu, and S. Gao, "Precursor ultrasonic effect on grain structure development of AA6061-T6 friction stir weld," *Materials & Design*, vol. 116, pp. 207–218, 2017.

[45] X. Lv, C. S. Wu, C. Yang, and G. K. Padhy, "Weld microstructure and mechanical properties in ultrasonic enhanced friction stir welding of Al alloy to Mg alloy," *Journal of Materials Processing Technology*, vol. 254, pp. 145–157, 2018, doi: 10.1016/j.jmatprotec.2017.11.031.

[46] M. N. Ilman, R. A. Sriwijaya, M. R. Muslih, and N. A. Triwibowo, "Strength and fatigue crack growth behaviours of metal inert gas AA5083-H116 welded joints under in-process vibrational treatment," *Journal of Manufacturing Processes*, vol. 59, pp. 727–738, 2020.

[47] J. Liu, H. Zhu, Z. Li, W. Cui, and Y. Shi, "Effect of ultrasonic power on porosity, microstructure, mechanical properties of the aluminum alloy joint by ultrasonic assisted laser-MIG hybrid welding," *Optics and Laser Technology*, vol. 119, no. 7089, p. 105619, 2019, doi: 10.1016/j.optlastec.2019.105619.

[48] T. Asami and H. Miura, "Ultrasonic welding of dissimilar metals by vibration with planar locus," *Acoustical Science and Technology*, vol. 36, no. 3, pp. 232–239, 2015.

[49] W. Xie, T. Huang, C. Yang, C. Fan, S. Lin, and W. Xu, "Comparison of microstructure , mechanical properties , and corrosion behavior of Gas Metal Arc (GMA) and Ultrasonic-wave-assisted GMA (U- GMA) welded joints of Al – Zn – Mg alloy," *Journal of Materials Processing Tech.*, vol. 277, no. October 2019, p. 116470, 2020, doi: 10.1016/j.jmatprotec.2019.116470.

[50] Y. Tian, J. Shen, S. Hu, Z. Wang, and J. Gou, "Effects of ultrasonic vibration in the CMT process on welded joints of Al alloy," *Journal of Materials Processing Technology*, vol. 259, pp. 282–291, 2018.

[51] G. Wang, M. S. Dargusch, M. Qian, D. G. Eskin, and D. H. StJohn, "The role of ultrasonic treatment in refining the as-cast grain structure during the solidification of an Al–2Cu alloy," *Journal of Crystal Growth*, vol. 408, pp. 119–124, 2014.

[52] B. M. Borkent, S. Gekle, A. Prosperetti, and D. Lohse, "Nucleation threshold and deactivation mechanisms of nanoscopic cavitation nuclei," *Physics of fluids*, vol. 21, no. 10, p. 102003, 2009.

[53] Q.-H. Chen, S.-B. Lin, C.-L. Yang, C.-L. Fan, and H.-L. Ge, "Effect of ultrasound on heterogeneous nucleation in TIG welding of Al–Li alloy," *Acta Metallurgica Sinica (English Letters)*, vol. 29, no. 12, pp. 1081–1088, 2016.

[54] R. Han, W. Dong, S. Lu, D. Li, and Y. Li, "Modeling of morphological evolution of columnar dendritic grains in the molten pool of gas tungsten arc welding," *Computational materials science*, vol. 95, pp. 351–361, 2014.

[55] Z. Lei, J. Bi, P. Li, Q. Li, Y. Chen, and D. Zhang, "Melt flow and grain refining in ultrasonic vibration assisted laser welding process of AZ31B magnesium alloy," *Optics & Laser Technology*, vol. 108, pp. 409–417, 2018.

[56] N. A. Muhammad and C. S. Wu, "Ultrasonic vibration assisted friction stir welding of aluminium alloy and pure copper," *Journal of Manufacturing Processes*, vol. 39, pp. 114–127, 2019.

[57] A. Ghahremaninezhad and K. Ravi-Chandar, "Ductile failure in polycrystalline OFHC copper," *International journal of solids and structures*, vol. 48, no. 24, pp. 3299–3311, 2011.

[58] L. Zhang and S. Zhang, "Using game theory to investigate the epigenetic control mechanisms of embryo development: Comment on:'Epigenetic game theory: How to compute the epigenetic control of maternal-to-zygotic transition' by Qian Wang et al.," *Physics of Life Reviews*, vol. 20, pp. 140–142, 2017.

[59] S. J. Fensin *et al.*, "Effect of loading direction on grain boundary failure under shock loading," *Acta Materialia*, vol. 64, pp. 113–122,

2014.
[60] S. Y. Tarasov, A. V Vorontsov, S. V Fortuna, V. E. Rubtsov, V. A. Krasnoveikin, and E. A. Kolubaev, "Ultrasonic-assisted laser welding on AISI 321 stainless steel," *Welding in the World*, vol. 63, no. 3, pp. 875–886, 2019.
[61] M. J. Jose, S. S. Kumar, and A. Sharma, "Vibration assisted welding processes and their influence on quality of welds," *Science and Technology of Welding and Joining*, vol. 21, no. 4, pp. 243–258, 2016.
[62] F. Yang, J. Zhou, and R. Ding, "Ultrasonic vibration assisted tungsten inert gas welding of dissimilar magnesium alloys," *Journal of Materials Science & Technology*, vol. 34, no. 12, pp. 2240–2245, 2018.
[63] D. Gao, Z. Li, Q. Han, and Q. Zhai, "Effect of ultrasonic power on microstructure and mechanical properties of AZ91 alloy," *Materials Science and Engineering: A*, vol. 502, no. 1–2, pp. 2–5, 2009.
[64] W. E. N. Tong, S. Liu, C. Shi, L. Liu, and Y. Chen, "Influence of high frequency vibration on microstructure and mechanical properties of TIG welding joints of AZ31 magnesium alloy," *Transactions of Nonferrous Metals Society of China*, vol. 25, no. 2, pp. 397–404, 2015.
[65] X. Jian, H. Xu, T. T. Meek, and Q. Han, "Effect of power ultrasound on solidification of aluminum A356 alloy," *Materials letters*, vol. 59, no. 2–3, pp. 190–193, 2005.
[66] S. Al-Ezzi, G. Quan, and A. Elrayah, "The mechanism of ultrasonic vibration on grain refining and Degassing in GTA spot welding of copper joints," *Materials*, vol. 11, no. 5, p. 737, 2018.
[67] A. Kostrivas and J. C. Lippold, "Fusion boundary microstructure evolution in aluminium alloys," *Welding in the World*, vol. 50, no. 11, pp. 24–34, 2006.
[68] M. M. Shtrikman, A. V Pinskii, A. A. Filatov, V. V Koshkin, E. A. Mezentseva, and N. V Guk, "Methods for reducing weld porosity in argon-shielded arc welding of aluminium alloys," *Welding International*, vol. 25, no. 06, pp. 457–462, 2011.
[69] V. Zohoori-Shoar, A. Eslami, F. Karimzadeh, and M. Abbasi-Baharanchi, "Resistance spot welding of ultrafine grained/nanostructured Al 6061 alloy produced by cryorolling process and evaluation of weldment properties," *Journal of Manufacturing Processes*, vol. 26, pp. 84–93, 2017.
[70] Q. Chen, S. Lin, C. Yang, C. Fan, and H. Ge, "Grain fragmentation in ultrasonic-assisted TIG weld of pure aluminum," *Ultrasonics sonochemistry*, vol. 39, pp. 403–413, 2017.
[71] W. D. Callister and D. G. Rethwisch, *Materials science and engineering: an introduction*, vol. 9. Wiley New York, 2018.
[72] Z. Yao *et al.*, "Acoustic softening and residual hardening in aluminum: modeling and experiments," *International Journal of Plasticity*, vol. 39, pp. 75–87, 2012.
[73] J. Wang, L. Jian, L. Qiang, and C. She, "Mechanical Analysis and Experimental Research on Ultrasonic Levitated Conical Rotor Piezoelectric Actuator," *International Journal of Applied Mechanics*, vol. 13, no. 03, p. 2150028, 2021.
[74] M. Ma, R. Lai, J. Qin, B. Wang, H. Liu, and D. Yi, "Effect of weld reinforcement on tensile and fatigue properties of 5083 aluminum metal inert gas (MIG) welded joint: Experiments and numerical simulations," *International Journal of Fatigue*, vol. 144, p. 106046, 2021.